IEEE Access
Multidisciplinary | Rapid Review | Open Access Journal

Received July 9, 2021, accepted July 17, 2021, date of publication July 20, 2021, date of current version July 27, 2021.

Digital Object Identifier 10.1109/ACCESS.2021.3098704

Wind Power Accommodation Method for Regional Integrated Heat-Power System Considering Generation and Load Uncertainties

DONGMEI YANG[1], ZHIHONG YANG[1], GUOXIN HE[1], JIAN GENG[1], AND JUNJIE LIGAO[2], (Member, IEEE)

[1]NARI Technology Company Ltd., Nanjing 211106, China
[2]School of Electrical and Automation, Wuhan University, Wuhan 430072, China

Corresponding author: Dongmei Yang (yangdongmei@sgepri.sgcc.com.cn)

This work was supported in part by the National Key Research and Development Program of China under Grant 2018YFB0905000, and in part by the Science and Technology Projects of State Grid Corporation of China under Grant SGTJDK00DWJS1800232.

ABSTRACT Due to the anti-peak shaving characteristics of wind power under the operation mode of ''power determined by heat'', a large number of wind power is abandoned at night. In order to solve the problem, this paper proposes a method of coordinated operation of ground source heat pump (GSHP) and combined heat and power (CHP) units. Through indirectly reducing the generation power of CHP units, the accommodation space of wind power in power grid is improved. A two-stage robust optimal scheduling model of regional integrated heat-power system (RIHPS) considering the uncertainty of wind power generation and power load is established. And a distributed solution method based on Alternating Direction Method of Multipliers (ADMM) method and column-and-constraint generation (C&CG) algorithm is designed. Then, the Locational marginal pricing strategy with the goal of guiding users to participate in wind power accommodation is analyzed. The numerical simulation results show that the wind power accommodation capacity of the integrated system under the operation mode of ''power determined by heat'' can be improved through installing GSHP at CHP units and using price signal guidance.

INDEX TERMS Power determined by heat, ground source heat pump, wind power accommodation, robust optimization, uncertainty.

NOMENCLATURE

INDEX AND SETS

n	Index of the buses of power system
p	Index of the nodes of heating system
v	Index of the electric boilers
w	Index of the ground source heat pumps
t	Index of the dispatching time steps
ref	Index of slack bus
l	Index of the number of iterations
$\boldsymbol{N}$	Set of the buses of power system
$\boldsymbol{L}$	Set of the branches of power system
$\boldsymbol{G}$	Set of the buses with generator units (including CHP units)
$\boldsymbol{M}$	Set of the nodes of heating system
$\boldsymbol{M}_S$	Set of the nodes with heat sources
$\boldsymbol{M}_{MIX}$	Set of the confluence nodes of heating system
$\boldsymbol{S}$	Set of the combined of heat and power units, electric boilers and ground source heat pumps
$\boldsymbol{T}$	Set of the dispatching time steps
$\boldsymbol{EB}$	Set of the electric boilers
$\boldsymbol{GSHP}$	Set of the ground source heat pumps
$\boldsymbol{CHP}$	Set of the combined of heat and power units
SE, SH	Set of the shared variables in the sub-problem of power system/heating system
$\boldsymbol{U}$	Set of the uncertain variables
$\boldsymbol{S}_p$	Set of water injection pipelines of node p

PARAMETERS

a, r	Day-ahead dispatching/real-time regulation cost of generator units
$\boldsymbol{B}$	Admittance matrix of power grid, and the element B_{ns} in it is the admittance of branch n-s
$W_{n,t}$	Output of wind turbines at bus n in time t

The associate editor coordinating the review of this manuscript and approving it for publication was Akshay Kumar Saha.

$D_{n,t}$ Power load at bus n in time t
$\overline{P_{ns}}$, $\underline{P_{ns}}$ Upper/lower bound of transmission power of branch n-s
$\overline{P_{n,t}}$ Upper limit of the output of generators at bus n in time t
$\overline{\theta_{n,t}}$, $\underline{\theta_{n,t}}$ Upper/lower bound of phase angle of voltage at bus n in time t
$\overline{\Delta_{n,t}}$, $\underline{\Delta_{n,t}}$ Upper/lower bound of the real-time regulation power at bus n in time t
$\overline{P_n^{EB}}$ Upper limit of the output of electric boilers at bus n in time t
$\overline{P_n^{GSHP}}$ Upper limit of the output of ground source heat pumps at bus n in time t
$\overline{U_{n,t}^W}$, $\underline{U_{n,t}^W}$ Upper/lower bounds of deviation between forecasted and actual wind power at bus n in time t
$\overline{U_{n,t}^D}$, $\underline{U_{n,t}^D}$ Upper/lower bounds of deviation between forecasted and actual power load at bus n in time t
$H_{p,t}^D$ Heating load at node p in time t
η_p^{EB} Energy conversion efficiency of electric boilers at node p
η_p^{GSHP} Energy conversion coefficient of ground source heat pumps at node p
c_p Specific heat capacity of water
λ_0, L_0 Heat transfer efficiency/length of the pipe
$T_{0,t}$ Normal temperature in time t
$\overline{H_{p,t}}$, $\underline{H_{p,t}}$ Upper/lower limit of the output of heat sources at node p in time t
$\overline{T_{p,t}}$, $\underline{T_{p,t}}$ Upper/lower bounds of the node temperature at node p in time t
$k_{CHP,n}$ Proportional coefficient of combined of heat and power units at bus n
ρ Penalty coefficient of quadratic term
ε_{pri}, $\varepsilon_{\text{dual}}$ Primitive/dual residual

VARIABLES

$P_{n,t}$ Output of generators at bus n in time t
$H_{p,t}$ Output of heat sources at node p in time t
$P_{v,t}^{EB}$ Output of electric boiler v in time t
$P_{w,t}^{GSHP}$ Output of ground source heat pump w in time t
$\Delta_{n,t}$ Real-time regulation power at bus n in time t
$\Delta W_{n,t}$ Abandoned wind power
$\theta_{n,t}$, $\theta_{n,t}^r$ Phase angle of voltage at bus n in time t during day-ahead dispatching/real-time regulation
$U_{n,t}^W$, $U_{n,t}^D$ Uncertain variables of wind power/power load at bus n in time t
$T_{p,t}^S$, $T_{p,t}^R$ Node temperature of water supply pipe and return pipe at node p in time t
m Mass flow rate
$T_{p,t}$ Node temperature at node p in time t
λ Lagrange multiplier

DUAL VARIABLES

$\lambda_{n,t}^P$, λ_t^{ref}, $\lambda_{n,t}^{rP}$, λ_t^{rref}, $\lambda_{p,t}^H$, $\lambda_{p,t}^T$, $\lambda_{p,t}^{MIX}$, $\mu_{ns,t}^{D-}$, $\mu_{ns,t}^{D+}$, $\mu_{n,t}^{G-}$, $\mu_{n,t}^{G+}$, $\mu_{n,t}^{\theta-}$, $\mu_{n,t}^{\theta+}$, $\mu_{ns,t}^{rL-}$, $\mu_{ns,t}^{rL-}$, $\mu_{ns,t}^{rL+}$, $\mu_{n,t}^{rG-}$, $\mu_{n,t}^{rG-}$, $\mu_{n,t}^{rG+}$, $\mu_{n,t}^{r-}$, $\mu_{n,t}^{r+}$, $\mu_{n,t}^{r\theta-}$, $\mu_{n,t}^{r\theta+}$, $\mu_{p,t}^{H-}$, $\mu_{p,t}^{H+}$, $\mu_{p,t}^{T-}$, $\mu_{p,t}^{T+}$.

ABBREVIATIONS

CHP	Combined heat and power
EB	Electric boiler
GSHP	Ground source heat pump
ADMM	Alternating Direction Method of Multipliers
C&CG	Column-and-constraint generation
LMP	Locational marginal pricing

I. INTRODUCTION

In the carbon emission gap report 2019, the United Nations Environment Programme (UNEP) pointed out that the global carbon emission needs to be reduced by 7.6% annually between 2020 and 2030 [1]. In the carbon emission gap report 2020, it pointed out that some departments need to realize the rapid transformation of decoupling with fossil fuels while improving energy efficiency [2]. It can be predicted that the installed capacity of renewable energy is expected to achieve double speed development in the future. In terms of wind power generation, the proportion of wind power generation in Denmark has reached 42% in 2015 [3], and the proportion of wind power generation in some states of the United States has also reached 30% in 2016 [4], among which the wind power penetration rate in Texas has reached 50% in some periods of 2017 [5]. With the increase of wind power installed capacity in the future, the proportion of wind power generation will further increase. However, although wind power is conducive to the goal of ''net zero emission'', the large-scale wind power and its uncertainty bring about the problems of wind power accommodation and the safe and stable operation of power grid, which become a major challenge for the power grid at present and in the future [6].

In order to solve the problem of wind power accommodation, Wu and Jiang [7] proposed the construction of energy storage system to improve the wind power adaptability of power grid. Zhang *et al.* [8] proposed a two-stage robust unit commitment model based on risk to analyze the acceptability of wind power, and Zhou *et al.* [9] proposed a quantitative method of operation risk caused by wind power uncertainty, which adapts to wind power by coordinating multi regional generation and reserve resources. Xu *et al.* [10] proposed that coordinating the spinning reserve of multiple regions will help to improve the adaptability of wind power generation, and established a game theory model of spinning reserve trading among regional systems, which regards spinning reserve as a commodity. Wei *et al.* [11] promoted the consumption of wind power by designing a reasonable trading mechanism for wind farms to participate in the market. Marketization is one of the effective means to solve the problem of renewable energy accommodation including wind power in the future.

At the same time, with the concept of energy Internet and integrated energy system [12], as well as a large number of energy conversion equipment such as combined heat and power (CHP) units and electric to gas equipment connected in different energy systems, the dependence between different energy systems is stronger. In this context, more and more scholars pay attention to promoting the accommodation of renewable energy such as wind power through the coordinated operation of different energy systems, which is worth studying. Fang *et al.* [13] proposed to use electric boiler (EB) with heat storage to participate in peak load regulation of power grid, so that the power grid can accommodate more wind power generation. Liang *et al.* [14] and Liu *et al.* [15] respectively analyzed the improvement effect of CHP unit and electric boiler equipped with heat storage device on the wind power accommodation capacity of integrated heat-power system. Through calculation, it showed that heat storage device and electric boiler can improve the wind power accommodation capacity and reduce coal consumption. Jiang *et al.* [16] and Chen *et al.* [17] used the flexibility of district heat system and natural gas system to promote the adaptation of integrated energy system to wind power generation by coordinating the energy production and consumption of different energy networks. The above references analyzed the methods to improve the wind power accommodation capacity of power system and integrated energy system, but there are two problems in these methods:

(1) The research scenarios designed were idealized. In some practical scenarios, for example, in the regional integrated heat-power system with CHP units as the core, due to the large proportion of micro-gas turbine power generation capacity and the anti-peak shaving characteristics of wind power, the system will have a serious problem of wind abandonment at night when the operation mode of ''power determined by heat'' is adopted in the heating season. The reason for this problem is that the system is limited by the operation mode of the CHP unit, which has not been analyzed in the existing references.

(2) When using market-oriented means to guide users to participate in wind power accommodation through price signals, the impact of wind power generation and power load uncertainty on pricing strategy is not considered at the same time.

Ground source heat pump (GSHP) technology is a new energy technology using shallow geothermal resources for heating [18], [19]. He *et al.* [20] proposed the idea of improving the peak load regulation capacity of thermal power units based on the cooperation of heat sources including electric boilers, heat pumps with thermal power units. Tseyzer *et al.* [21] established the mathematical model of the joint work of heat pump and thermal power plant, and analyzed the feasibility of the joint work. Gao *et al.* [22] analyzed the economy of heat pump participating in combined cooling, heating and power (CCHP). Through calculation, it showed that heat pump can effectively reduce the energy system cost and waste wind power within a certain capacity range. Yang *et al.* [23] proposed the optimal operation model of the integrated heat-power system with the participation of heat pumps and CHP units, and designed a distributed solution algorithm based on the two-step hydraulic-thermal decomposition method. The results showed that the interaction between the power grid and the heat supply network can improve the wind power accommodation capacity of the system. Arcuri *et al.* [24] proposed the method of photovoltaics and heat pumps participating in the demand response of micro grid, and verified it with the actual scene in the University of Calabria. In the existing literature, a large number of scholars have studied the optimal operation of power system and integrated energy system with the participation of heat pumps. The research results show that heat pumps can indeed improve the wind power accommodation ability of the system. However, in these research results, the role of heat pump is only as a power load, which consumes electricity to improve the space of wind power accommodation. There is a lack of analysis on the effect of the cooperative operation mode of heat pumps and CHP units on the improvement of wind power accommodation capacity of the system.

At present, a lot of scholars have studied the pricing methods of power system operators. The mainstream pricing method is the locational marginal pricing (LMP) method of Pennsylvania-New Jersey-Maryland (PJM) electricity wholesale market in the United States [25]. On the basis of LMP of transmission level wholesale market, the distribution locational marginal pricing (DLMP) method of distribution level wholesale market with distributed generations (DGs) is proposed in references [26]–[28]. The actual practice of PJM electricity wholesale market and the simulation results in the literature show that the pricing method based on LMP can guide users to participate in peak load regulation and reduce the risk of grid congestion. Yue *et al.* [29] proposed a joint clearing mechanism of electricity market and heat market based on LMP of electricity market, and studied the impact of electricity load and heat load demand on market price. However, only a single time section is considered in this reference. For the uncertainty of generation and load, Fang *et al.* [30] proposed a clearing mechanism of electricity market based on LMP. LMP reflected the system cost caused by the uncertainty of generation and load demand in different locations. The existing research results of operator pricing methods mainly focus on the deterministic operation scenarios, that is, the renewable energy such as wind power and photovoltaic is not considered or the uncertainty is ignored, and the energy market is dominated by the power market. There is a lack of research on pricing method of integrated energy system operation scenario under generation and load uncertainty.

In the aspect of solving the uncertainty problem in the power system and integrated heat-power system, many insightful methods and models have been proposed. Lu *et al.* [31] considered the uncertainties of the net electrical-load and outdoor temperature, and then a day-ahead adaptive robust dispatch model and corresponding

linearization method were proposed. The uncertainties including building parameters, weather factors, and human behavior were also modeled and considered in [32]. Reddy *et al.* [33] used the ''best-fit'' participation factors to find the optimal real-time schedules considering the uncertainty of renewable energy resources. A two stage optimal schedule strategy consisted of a genetic algorithm based day-ahead optimum scheduling and a two-point estimate based probabilistic real time optimal power flow was proposed in [34] and [35]. In addition, an informative differential evolution with self-adaptive re-clustering technique was proposed to solve the optimal scheduling problem of a wind-thermal power system in [36]. And then the trade-off between cost and emission minimization objectives for the wind-thermal power system was showed in [37]. Nosratabadi *et al.* [38] proposed a robust scenario-based optimization strategy to deal with the uncertainty from market price, wind power output and plug-in hybrid electric vehicles. Similarly, Zafarani *et al.* [39] presented a bounded uncertainty-based robust optimization and Nojavan *et al.* [40] proposed a risk-constrained scheduling model to solve the uncertainty problem in CHP-based microgrid. The above methods provide important reference for the solution of uncertainty in integrated heat-power system.

To sum up, there are two main problems in the existing research results of wind power accommodation:

(1) There is a lack of analysis on the effect of the coordinated operation of heat pumps and CHP units on the improvement of wind power accommodation capacity of the integrated heat-power system under the mainstream operation mode of ''power based on heat''.

(2) The impact of generation and load uncertainty and multi energy system interaction on the LMP has not been considered.

The operation mode of ''power determined by heat'' is the main operation mode of integrated heat-power system at present. On the premise of not changing this mode, how to use the existing resources to absorb wind power to the maximum extent is worth studying. At the same time, wind power with high permeability on the generation side has natural strong intermittence and fluctuation. The power load on the load side presents a diversified development, its fluctuation is increasing and changing rule is difficult to grasp. It is inevitable that there will be deviations when the system operator forecast the next-day wind power and power load, which will have a significant impact on the actual scheduling results. Therefore, under the double uncertainties from generation side and load side, how to make the optimal pricing strategy of power grid to guide users to participate in wind power accommodation is also a difficult problem. The contributions of this paper are as follows:

(1) The methods of configuring low cost GSHPs at the CHP unit and price signal guidance based on the locational marginal pricing are proposed to solve the serious wind abandonment problem of the regional integrated heat-power system with the operation mode of ''power determined by heat''. The GSHPs can share the heating load of the CHP unit, thus reducing the power generation of the CHP unit and increasing the accommodation space of wind power. The price signal can shift the daytime load to night to increase the nighttime load. These two methods can solve the wind power accommodation problem effectively.

(2) A two-stage robust optimal scheduling model of regional integrated heat-power system considering the double uncertainties of generation and load is established to analyze the impact of the double uncertainties on the locational marginal pricing. Based on the model, the impact of double uncertainties on locational marginal pricing is found, that is, the increase of uncertainty will lead to the increase of peak-valley difference of locational marginal price. And then, three methods including increasing the capacity of GSHPs, reducing the proportional coefficient of CHPs and increasing the energy conversion coefficient of GSHPs are proposed to solve the wind power abandonment problem caused by the insufficient transmission capacity.

(3) A method based on Alternating Direction Method of Multipliers (ADMM) and column-and-constraint generation (C&CG) is proposed to reduce the scale and complexity of the model. The performance of the distributed algorithm proposed in this paper is tested. The test results show that the algorithm can solve the two-stage robust optimal scheduling model quickly when the branch transmission capacity is sufficient. Although the insufficient branch transmission capacity in power system will increase the number of iterations and consuming time, the algorithm is still feasible and has good convergence.

II. OPTIMIZATION FRAMEWORK

When the wind power in the regional integrated heat-power system presents the characteristics of low valley in the daytime and high peak at night, the CHP units need to follow the change of heat load at all times and cannot participate in the power supply regulation independently under the operation mode of ''power determined by heat''. Therefore, the CHP unit still needs to maintain a large output during the period of high heating load at night. However, at the same time, the power load on the grid side is in a low period, which will lead to a large number of abandoned wind at night. In order to solve the problem of abandoning wind at night, the following two methods can be used:

(1) When there are abundant shallow geothermal resources in the area, GSHPs can be installed at the nodes with CHP units on the heating network side. Through reducing the heat load of CHP units at night, the generating power of CHP units can be reduced to increase the accommodation space of wind power.

(2) The power grid operator guides power users to shift part of the daytime load to nighttime load by setting the LMP of each period. Maximize the power load at night and reduce the amount of abandoned wind power.

Combined with the above two methods, the wind power accommodation framework of the regional integrated heat-power system is established, as shown in Figure 1. In the

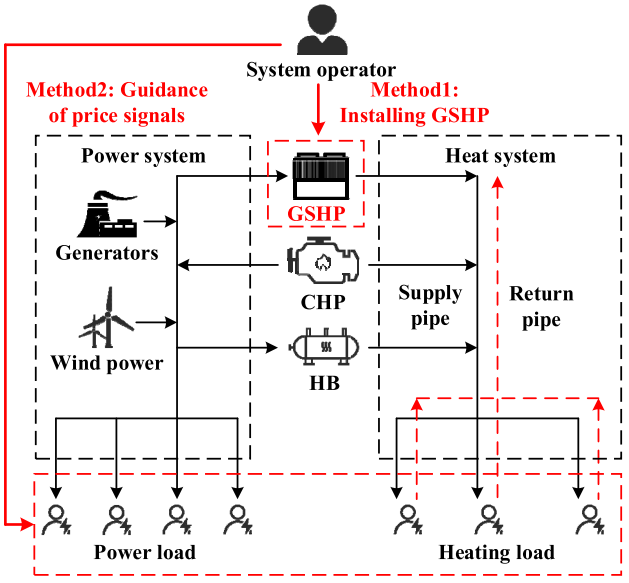

FIGURE 1. Wind power accommodation framework of regional integrated heat-power system.

framework, the power grid and heating network are coupled by the CHP unit, the electric boiler (EB) and the GSHP. Among them, CHP unit consumes natural gas to generate a fixed proportion of electric energy and heat energy to supply to the integrated system. The EB and the GSHP consume electric energy and convert it into heat energy to supply to the heating network.

III. MODELING AND DECOMPOSITION

A. ROBUST OPTIMIZATION MODEL

Firstly, the optimization model of centralized scheduling mode is established. The regional integrated heat-power system is composed of power system and heat system, so the operation cost and related constraints of power grid and heating network should be considered when making dispatching schedule. Due to the uncertainty of wind power on the generation side and power load on the load side, it is necessary to con-sider the regulation cost of generator units in the real-time dispatching stage on the basis of day ahead operation cost. Therefore, the objective function of the centralized scheduling model is as follows:

$$\begin{aligned}\min & \sum_{t\in \boldsymbol{T}}\sum_{n\in \boldsymbol{G}} a_n P_{n,t} + \sum_{t\in \boldsymbol{T}}\sum_{p\in \boldsymbol{M}} a_p H_{p,t} \\ & + \sum_{t\in \boldsymbol{T}}\sum_{v\in \boldsymbol{EB}} a_v P^{EB}_{v,t} + \sum_{t\in \boldsymbol{T}}\sum_{w\in \boldsymbol{GSHP}} a_w P^{GSHP}_{w,t} \\ & + \max_{U^W_{n,t},U^D_{n,t}} \min_{\Delta_{n,t}} \sum_{t\in \boldsymbol{T}}\sum_{n\in \boldsymbol{G}} r_n \Delta_{n,t} \end{aligned} \tag{1}$$

On the grid side, the following constraints can be obtained based on the direct-current (DC) power flow model:

$$\begin{aligned} & P_{n,t} + W_{n,t} - \Delta W_{n,t} - D_{n,t} - P^{EB}_{n,t} - P^{GSHP}_{n,t} \\ & \quad = \sum_{s:n\to s} B_{ns}\left(\theta_{n,t} - \theta_{s,t}\right) : \lambda^P_{n,t}, \quad \forall n, s \in \boldsymbol{N} \end{aligned} \tag{2}$$

$$\underline{P_{ns}} \le B_{ns}\left(\theta_{n,t} - \theta_{s,t}\right) \le \overline{P_{ns}} : \mu^{D-}_{ns,t}, \mu^{D+}_{ns,t}, (n,s) \le \boldsymbol{L} \tag{3}$$

$$0 \le P_{n,t} \le \overline{P_{n,t}} : \mu^{G-}_{n,t}, \mu^{G+}_{n,t}, \quad \forall n \in \boldsymbol{G} \tag{4}$$

$$\underline{\theta_{n,t}} \le \theta_{n,t} \le \overline{\theta_{n,t}} : \mu^{\theta-}_{n,t}, \mu^{\theta+}_{n,t}, \quad \forall n \in \boldsymbol{N} \tag{5}$$

$$\theta_{ref,t} = 0 : \lambda^{ref}_t, n = ref \tag{6}$$

$$\begin{aligned} & P_{n,t} + \left(W_{n,t} + U^W_{n,t}\right) - \Delta W_{n,t} \\ & \quad - \left(D_{n,t} + U^D_{n,t}\right) - P^{EB}_{n,t} - P^{GSHP}_{n,t} + \Delta_{n,t} \\ & \quad = \sum_{s:n\to s} B_{ns}\left(\theta^r_{n,t} - \theta^r_{s,t}\right) : \lambda^{rP}_{n,t}, \quad \forall n, s \in \boldsymbol{N} \end{aligned} \tag{7}$$

$$\underline{P_{ns}} \le B_{ns}\left(\theta^r_{n,t} - \theta^r_{s,t}\right) \le \overline{P_{ns}} : \mu^{rL-}_{ns,t}, \mu^{rL+}_{ns,t}, (n,s) \in \boldsymbol{L} \tag{8}$$

$$0 \le P_{n,t} + \Delta_{n,t} \le \overline{P_{n,t}} : \mu^{rG-}_{n,t}, \mu^{rG+}_{n,t}, \quad \forall n \in \boldsymbol{G} \tag{9}$$

$$\underline{\Delta_{n,t}} \le \Delta_{n,t} \le \overline{\Delta_{n,t}} : \mu^{r-}_{n,t}, \mu^{r+}_{n,t}, \quad \forall n \in \boldsymbol{G} \tag{10}$$

$$\underline{\theta_{n,t}} \le \theta^r_{n,t} \le \overline{\theta_{n,t}} : \mu^{r\theta-}_{n,t}, \mu^{r\theta+}_{n,t}, \quad \forall n \in \boldsymbol{N} \tag{11}$$

$$\theta^r_{ref,t} = 0 : \lambda^{rref}_t, \quad n = ref \tag{12}$$

$$0 \le P^{EB}_{n,t} \le \overline{P^{EB}_n}, \quad n \in \boldsymbol{EB} \tag{13}$$

$$0 \le P^{GSHP}_{n,t} \le \overline{P^{GSHP}_n}, \quad n \in \boldsymbol{GSHP} \tag{14}$$

$$\boldsymbol{U} = \left\{ U^W_{n,t}, U^D_{n,t} \,\middle|\, \begin{array}{l} \underline{U^W_{n,t}} \le U^W_{n,t} \le \overline{U^W_{n,t}}, \\ \underline{U^D_{n,t}} \le U^D_{n,t} \le \overline{U^D_{n,t}} \end{array} \right\} \tag{15}$$

where (n, s) denotes branch n-s, n and s are the start and end buses respectively. The dual variable $\lambda^P_{n,t}$ is the day-ahead locational marginal price of bus n at time t. Formula (2)-(6) are the constraints of day-ahead dispatching stage. Formula (7)-(12) are the constraints of real-time dispatching stage. Formula (13)-(14) are the heating power constraints of EBs and GSHPs. Formula (15) is the uncertain set of wind power output and electric load. In this uncertain set, the range constraints of wind power and power load forecasting deviations in each period are given. The upper and lower bounds of constraints can be derived from the probability distributions obtained from historical data.

On the heating network side, the heating load is mostly residential heating load, which has strong regularity and small fluctuation. Therefore, this paper assumes that the heating load is deterministic. The heating supply and return network structure adopted in this paper is shown in Figure 2. The heating network consists of heat sources, heating loads, water supply pipes and return pipes.

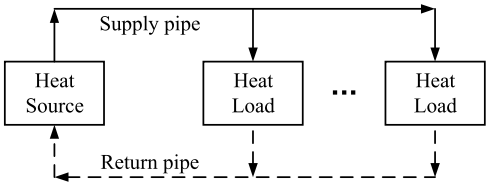

FIGURE 2. Schematic diagram of heating network structure.

Based on the thermodynamic model including water supply network and return network, the following constraints can be obtained:

$$H_{p,t} + \eta_p^{EB} P_{p,t}^{EB} + \eta_p^{GSHP} P_{p,t}^{GSHP} - H_{p,t}^{D} = c_p m \left(T_{p,t}^{S} - T_{p,t}^{R}\right) : \lambda_{p,t}^{H}, \quad \forall p \in \boldsymbol{M} \tag{16}$$

$$T_{q,t} = \left(T_{p,t} - T_{0,t}\right) e^{-\frac{\lambda_0 L_0}{c_p m}} + T_{0,t} : \lambda_{p,t}^{T}, \quad \forall p, q \in \boldsymbol{M} \tag{17}$$

$$T_{p,t} \sum_{\omega \in \boldsymbol{S}_p} m_\omega = \sum_{\omega \in \boldsymbol{S}_p} m_\omega T_{\omega,t} : \lambda_{p,t}^{MIX}, \quad \forall p \in \boldsymbol{M}_{MIX} \tag{18}$$

$$\underline{H_{p,t}} \le H_{p,t} \le \overline{H_{p,t}} : \mu_{p,t}^{H-}, \mu_{p,t}^{H+}, \quad \forall p \in \boldsymbol{M}_S \tag{19}$$

$$\underline{T_{p,t}} \le T_{p,t} \le \overline{T_{p,t}} : \mu_{p,t}^{T-}, \mu_{p,t}^{T+}, \quad \forall p \in \boldsymbol{M} \tag{20}$$

where the dual variable $\lambda_{p,t}^{H}$ is the locational marginal heat price of node p at time t. Formula (16) is the node balance constraint. Formula (17) is the constraint of pipe temperature drop. By assuming constant mass flow rate m, (17) becomes a linear constraint. That is, the temperature at node p is a linear function of temperature at node q. Formula (18) is the constraint of the confluence node. Formula (19) and (20) are the constraints of heat source output and node temperature.

The CHP is the key coupling part between power grid and heating network, and its heating power and generating power meet the following proportional relationship:

$$P_{n,t} = k_{CHP,n} H_{n,t}, \quad \forall n \in \boldsymbol{CHP} \tag{21}$$

B. MODEL DECOMPOSITION

As the robust optimization model of formulas (1)-(21) contains a large number of variables in the power grid and heating network, the solution complexity is large. Therefore, the Alternating Direction Method of Multipliers (ADMM) algorithm [31] is introduced to decompose the above robust optimization problem into power system robust optimization sub-problem and heat system deterministic optimization sub-problem. The decomposition principle is shown in Figure 3. The basic idea of decomposition is as follows: generating power P of CHPs, heating power P^{EB} of EBs and heating power P^{GSHP} of GSHPs are used as the shared variables of power system and heat system. The shared variables are transferred between the two systems and the Lagrange multiplier λ is updated. After a few but many times of information transmission, the global optimization is achieved. The specific model after decomposition is as follows.

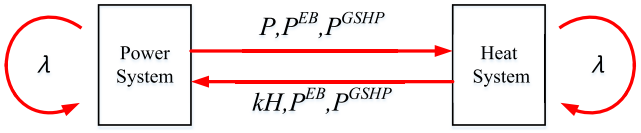

FIGURE 3. Schematic diagram of ADMM algorithm decomposition mechanism.

The sub-problem of power system is as follow:

$$\begin{aligned}\min & \sum_{t \in \boldsymbol{T}} \sum_{n \in \boldsymbol{G}} a_n P_{n,t} + \sum_{t \in \boldsymbol{T}} \sum_{v \in \boldsymbol{EB}} a_v P_{v,t}^{EB} + \sum_{t \in \boldsymbol{T}} \sum_{w \in \boldsymbol{GSHP}} a_w P_{w,t}^{GSHP} \\ & + \sum_{t \in \boldsymbol{T}} \sum_{n \in \boldsymbol{S}} \lambda_{n,t}^{(l)} \left(SE_{n,t} - SH_{n,t}^{(l)}\right) \\ & + \frac{\rho}{2} \sum_{t \in \boldsymbol{T}} \sum_{n \in \boldsymbol{S}} \left\| SV_{n,t} - SV_{n,t}^{(l)} \right\|_2^2 \\ & + \max_{U_{n,t}^{W}, U_{n,t}^{D}} \min_{\Delta_{n,t}} \sum_{t \in \boldsymbol{T}} \sum_{n \in \boldsymbol{G}} r_n \Delta_{n,t} \end{aligned} \tag{22}$$

$$s.t.\ (2) - (15),$$

$$SE = \left\{P, P^{EB}, P^{GSHP}\right\}, \quad \boldsymbol{S} = \{\boldsymbol{CHP}, \boldsymbol{EB}, \boldsymbol{GSHP}\} \tag{23}$$

The sub-problem of heat system is as follow:

$$\begin{aligned}\min & \sum_{t \in \boldsymbol{T}} \sum_{p \in \boldsymbol{M}} a_p H_{p,t} + \sum_{t \in \boldsymbol{T}} \sum_{p \in \boldsymbol{S}} \lambda_{p,t}^{(l)} \left(SE_{p,t}^{(l+1)} - SH_{p,t}\right) \\ & + \frac{\rho}{2} \sum_{t \in \boldsymbol{T}} \sum_{n \in \boldsymbol{S}} \left\| SV_{p,t}^{(l+1)} - SV_{p,t} \right\|_2^2 \end{aligned} \tag{24}$$

$$s.t.\ (16) - (20),$$

$$SH = \left\{k_{CHP} H, P^{EB}, P^{GSHP}\right\}, \quad \boldsymbol{S} = \{\boldsymbol{CHP}, \boldsymbol{EB}, \boldsymbol{GSHP}\} \tag{25}$$

The calculation steps of ADMM algorithm are as follows:

Step 1: Set the number of iterations $l = 1$. Given the primitive residual ε_{pri}, dual residual $\varepsilon_{\text{dual}}$ and penalty coefficient ρ. Set the initial value of the shared variable $SE^{(0)}$a nd the initial value of Lagrange multiplier $\lambda^{(0)}$.

Step 2: Solve the power system sub-problem formula (22)-(23) and the heat system sub-problem formula (24)-(25) successively, and update the Lagrange multiplier λ according to the following formula (26).

$$\lambda_{n,t}^{(l+1)} = \lambda_{n,t}^{(l)} + \rho \left(SE_{n,t}^{(l+1)} - SH_{n,t}^{(l+1)}\right) \tag{26}$$

Step 3: Judge the convergence according to formula (27) and (28). If the convergence criterion is established, stop the calculation and output the results. Otherwise, set $l = l+1$ and go to Step 2 to start the next serial iterative optimization calculation.

$$\left\| SE_{n,t}^{(l+1)} - SH_{n,t}^{(l+1)} \right\|_2^2 \le \varepsilon_{\text{pri}} \tag{27}$$

$$\left\| SE_{n,t}^{(l+1)} - SE_{n,t}^{(l)} \right\|_2^2 \le \varepsilon_{\text{dual}} \tag{28}$$

C. COLUMN-AND-CONSTRAINT GENERATION ALGORITHM

The power system sub-problem formula (24)-(25) is now rewritten in a compact form (29). It can be seen that the problem is an optimization problem in the form of min-max-min, and its multi-layer characteristics make it difficult to solve the problem directly.

$$\min_{x} \left(c^T x + \max_{d \in \boldsymbol{D}} \min_{y} b^T y\right)$$

$$\begin{aligned} s.t.\ & Fx \le f \\ & Ax + By \le g \\ & Hy \le h \\ & I_u y = d \\ & \boldsymbol{D} = \{d \mid Ed \le e\} \end{aligned} \tag{29}$$

where x is the day-ahead dispatching schedule. y is the real-time regulation power, and $\boldsymbol{D}$ is the set of uncertain variables.

The column-and-constraint generation(C&CG) algorithm is introduced to solve the two-stage robust optimization problem formula (29). The algorithm reduces the scale of problem solving by decomposing the problem. After decomposition, the original problem can be represented as a sub-problem (SP) and a main-problem (MP). The MP is as follow:

$$\begin{aligned} \min_{x,\alpha}\ & \left(c^T x + \alpha\right) \\ s.t.\ & Fx \le f \\ & \alpha \ge b^T y^z, \quad \forall z \in \boldsymbol{O} \\ & Ax + By^z \le g, \quad \forall z \le l \\ & Hy^z \le h, \quad \forall z \le l \\ & I_u y^z = d, \quad \forall z \le l \end{aligned} \tag{30}$$

where $\boldsymbol{O}$ is the set of feasible solutions. l is the number of iterations. z is the index of feasible solutions.

In the SP, the original problem is in min-max form. When solving the SP, the day-ahead dispatching schedule x is the determined value after solving the MP, which can be regarded as parameters. For min-max problem, dual theory is used to transform the min-form optimization problem into max-form optimization problem. The inner optimization problem is as follow:

$$\begin{aligned} \min_{y}\ & b^T y \\ s.t.\ & By \ge g - Ax : \lambda \\ & Hy \ge h : \varphi \\ & I_u y = d : \eta \end{aligned} \tag{31}$$

The duality of equation (31) is as follow. In this problem, the uncertain variable set $\boldsymbol{D}$ and the day-ahead dispatching schedule x are the parameters of the problem, rather than the constraint variables. The optimal value of the problem can be considered as a function of the uncertain variable set $\boldsymbol{D}$ and the day-ahead dispatching schedule x.

$$\begin{aligned} S(x,d) = \max_{\lambda,\varphi,\eta}\ & \lambda^T (Ax - g) - \varphi^T h + \eta^T d \\ s.t.\ & -\lambda^T B - \varphi^T h + \eta^T d = b^T \\ & \varphi \ge 0, \lambda \ge 0, \eta\ free \end{aligned} \tag{32}$$

After introducing the outer max-problem of the sub-problem, it is shown in formula (33). At this point, Lagrange multipliers and uncertain variable set $\boldsymbol{D}$ are new decision variables, and the day-ahead dispatching schedule x is the parameter.

$$\begin{aligned} R(x,d) = \max_{\lambda,\varphi,\eta,d}\ & \lambda^T (Ax - g) - \varphi^T h + \eta^T d \\ s.t.\ & -\lambda^T B - \varphi^T h + \eta^T d = b^T \\ & \varphi \ge 0, \lambda \ge 0, \eta\ free \\ & d \in \boldsymbol{D} \end{aligned} \tag{33}$$

Based on the above decomposition results, the specific calculation steps of C&CG algorithm are as follows:

Step 1: Set the solution accuracy ε, iteration number $l = 1$, feasible solution set $O = \emptyset$, upper bound UB= $+\infty$, lower bound LB =$-\infty$.

Step 2: Solve the MP (30). Note that the feasible solutions are x_{l+1} and α_{l+1}, and the lower bound of the new estimation is LB= $c^{\mathrm{T}} x_l + \alpha_l$.

Step 3: Solve the SP (33). Note that the result is $R(x_l)$, and the upper bound of the new estimation is UB=max$\{c^{\mathrm{T}} x_l + R(x_l)$, UB$\}$.

Step 4: if UB-LB$\le\ \varepsilon$, x_l is the optimal solution of the problem, and the calculation ends. Otherwise, perform the following steps:

(1) If $R(x_l) < +\infty$, a new variable y^{z+1} is added to the original problem, and the following constraints are added to the original problem.

$$\begin{aligned} & \alpha \ge b^T y^{z+1} \\ & Ax + By^{z+1} \le g \\ & Hy^{z+1} \le h \\ & I_u y^{z+1} = d \end{aligned} \tag{34}$$

Execute $\boldsymbol{O}$=$\boldsymbol{O}\cup\{z+1\}$, $z = z+1$ and go to Step 2.

(2) If $R(x_l) = +\infty$, add a new variable y^{z+1} to the original main problem, and the following constraints are added to the original problem. The indeterminate variable d here can be calculated by introducing a relaxation variable in sub-problem (33) and using the method in [42].

$$\begin{aligned} & Ax + By^{z+1} \le g \\ & Hy^{z+1} \le h \\ & I_u y^{z+1} = d \end{aligned} \tag{35}$$

Execute $z = z+1$ and go to Step 2.

Therefore, based on the above decomposition method, the main problem and the sub-problem obtained from equation (22)-(23) are as follows.

$$\begin{aligned} \mathbf{MP}: \min_{P_{n,t}}\ & \sum_{t\in\boldsymbol{T}}\sum_{n\in\boldsymbol{G}} a_n P_{n,t} + \sum_{t\in\boldsymbol{T}}\sum_{v\in\boldsymbol{EB}} a_v P_{v,t}^{EB} \\ & + \sum_{t\in\boldsymbol{T}}\sum_{w\in\boldsymbol{GSHP}} a_w P_{w,t}^{GSHP} \\ & + \sum_{t\in\boldsymbol{T}}\sum_{n\in\boldsymbol{S}} \lambda_{n,t}^{(l)} \left(SE_{n,t} - SH_{n,t}^{(l)}\right) \\ & + \frac{\rho}{2}\sum_{t\in\boldsymbol{T}}\sum_{n\in\boldsymbol{S}} \left\| SV_{n,t} - SV_{n,t}^{(l)} \right\|_2^2 + \alpha \\ s.t.\ & (23), \\ & \alpha \ge \sum_{t\in T}\sum_{n\in G} r_n \Delta_{n,t} \end{aligned} \tag{36}$$

$$
\begin{aligned}
\mathbf{SP}: \max_{\Delta_{n,t},\boldsymbol{U}} & -\sum_{t\in\boldsymbol{T}}\sum_{n\in\boldsymbol{G}}\lambda_{n,t}^{rP}\begin{pmatrix}P_{n,t}+W_{n,t}-\Delta W_{n,t}\\-D_{n,t}-P_{n,t}^{EB}-P_{n,t}^{GSHP}\end{pmatrix}\\
&-\sum_{t\in\boldsymbol{T}}\sum_{n\in\boldsymbol{N}\backslash\boldsymbol{G}}\lambda_{n,t}^{rP}\begin{pmatrix}W_{n,t}-\Delta W_{n,t}\\-D_{n,t}-P_{n,t}^{EB}-P_{n,t}^{GSHP}\end{pmatrix}\\
&-\sum_{t\in\boldsymbol{T}}\sum_{n\in\boldsymbol{N}}\lambda_{n,t}^{rP}\left(U_{n,t}^{W}-U_{n,t}^{D}\right)\\
&+\sum_{t\in\boldsymbol{T}}\sum_{(n,s)\in\boldsymbol{L}}\mu_{ns,t}^{rL-}\underline{P_{ns}}-\sum_{t\in\boldsymbol{T}}\sum_{(n,s)\in\boldsymbol{L}}\mu_{ns,t}^{rL+}\overline{P_{ns}}\\
&+\sum_{t\in\boldsymbol{T}}\sum_{n\in\boldsymbol{G}}\mu_{n,t}^{rG-}\left(-P_{n,t}\right)\\
&-\sum_{t\in\boldsymbol{T}}\sum_{n\in\boldsymbol{G}}\mu_{n,t}^{rG+}\left(\overline{P_{n,t}}-P_{n,t}\right)\\
&+\sum_{t\in\boldsymbol{T}}\sum_{n\in\boldsymbol{G}}\mu_{n,t}^{r-}\underline{\Delta_{n,t}}-\sum_{t\in\boldsymbol{T}}\sum_{n\in\boldsymbol{G}}\mu_{n,t}^{r+}\overline{\Delta_{n,t}}\\
&+\sum_{t\in\boldsymbol{T}}\sum_{n\in\boldsymbol{N}}\mu_{n,t}^{r\theta-}\underline{\theta_{n,t}^{r}}-\sum_{t\in\boldsymbol{T}}\sum_{n\in\boldsymbol{N}}\mu_{n,t}^{r\theta+}\overline{\theta_{n,t}^{r}} \qquad (37)\\
s.t.\ & \frac{\partial L}{\partial\Delta_{n,t}}=r_{n,t}-\lambda_{n,t}^{rP}-\mu_{n,t}^{rG-}+\mu_{n,t}^{rG+}-\mu_{n,t}^{r-}\\
&+\mu_{n,t}^{r+}=0,\ n\in\boldsymbol{G}\\
\frac{\partial L}{\partial\theta_{n,t}}=&\begin{cases}\begin{pmatrix}-\lambda_{n,t}^{rP}\sum\limits_{s:n\to s}B_{ns}+\sum\limits_{s:n\to s}\lambda_{s,t}^{rP}B_{ns}\\-\sum\limits_{s:n\to s}\mu_{ns,t}^{rL-}B_{ns}+\sum\limits_{s:n\to s}\mu_{sn,t}^{rL-}B_{sn}\\-\sum\limits_{s:n\to s}\mu_{sn,t}^{rL+}B_{sn}+\sum\limits_{s:n\to s}\mu_{ns,t}^{rL+}B_{ns}\\-\mu_{n,t}^{r\theta-}+\mu_{n,t}^{r\theta+}+\lambda_{t}^{rref}\end{pmatrix}=0,\\ n\in ref\\ \begin{pmatrix}-\lambda_{n,t}^{rP}\sum\limits_{s:n\to s}B_{ns}+\sum\limits_{s:n\to s}\lambda_{s,t}^{rP}B_{ns}\\-\sum\limits_{s:n\to s}\mu_{ns,t}^{rL-}B_{ns}+\sum\limits_{s:n\to s}\mu_{sn,t}^{rL-}B_{sn}\\-\sum\limits_{s:n\to s}\mu_{sn,t}^{rL+}B_{sn}+\sum\limits_{s:n\to s}\mu_{ns,t}^{rL+}B_{ns}\\-\mu_{n,t}^{r\theta-}+\mu_{n,t}^{r\theta+}\end{pmatrix}=0,\\ n\in\boldsymbol{N}\backslash ref\end{cases}\\
&\mu_{mn,t}^{rL-},\mu_{mn,t}^{rL+}\geq 0,\ \mu_{n,t}^{r\theta-},\mu_{n,t}^{r\theta+}\geq 0,\ \mu_{n,t}^{G-},\mu_{n,t}^{G+}\geq 0,\\
&\mu_{n,t}^{rG-},\mu_{n,t}^{r+}\geq 0,\ \mu_{n,t}^{r-},\mu_{n,t}^{r+}\geq 0,\\
\boldsymbol{U}=&\left\{U_{n,t}^{W},U_{n,t}^{D}\ \middle|\ \begin{matrix}\underline{U_{n,t}^{W}}\leq U_{n,t}^{W}\leq\overline{U_{n,t}^{W}},\\ \underline{U_{n,t}^{D}}\leq U_{n,t}^{D}\leq\overline{U_{n,t}^{D}}\end{matrix}\right\} \qquad (38)\\
&\sum_{t\in\boldsymbol{T}}\sum_{n\in\boldsymbol{N}}\lambda_{n,t}^{rP}\left(U_{n,t}^{W}-U_{n,t}^{L}\right)\\
=&\sum_{t\in\boldsymbol{T}}\sum_{n\in\boldsymbol{N}}\begin{bmatrix}U_{n,t}^{W,\mathrm{b}}\beta_{n,t}^{\mathrm{b}}+\left(U_{n,t}^{W,\mathrm{b}}+\overline{U_{n,t}^{W}}\right)\beta_{n,t}^{+}\\+\left(U_{n,t}^{W,\mathrm{b}}+\underline{U_{n,t}^{W}}\right)\beta_{n,t}^{-}\end{bmatrix}\\
&-\sum_{t\in\boldsymbol{T}}\sum_{n\in\boldsymbol{N}}\begin{bmatrix}U_{n,t}^{D,\mathrm{b}}\gamma_{n,t}^{\mathrm{b}}+\left(U_{n,t}^{D,\mathrm{b}}+\overline{U_{n,t}^{D}}\right)\gamma_{n,t}^{+}\\+\left(U_{n,t}^{D,\mathrm{b}}+\underline{U_{n,t}^{D}}\right)\gamma_{n,t}^{-}\end{bmatrix} \qquad (39)\\
s.t.\ & \lambda_{n,t}^{rP}=\beta_{n,t}^{\mathrm{base}}+\beta_{n,t}^{+}+\beta_{n,t}^{-}\\
&\lambda_{n,t}^{rP}=\gamma_{n,t}^{\mathrm{base}}+\gamma_{n,t}^{+}+\gamma_{n,t}^{-}\\
&\mu_{n,t}^{\mathrm{base}}+\mu_{n,t}^{+}+\mu_{n,t}^{-}=1\\
&\kappa_{n,t}^{\mathrm{base}}+\kappa_{n,t}^{+}+\kappa_{n,t}^{-}=1\\
&-\mu_{n,t}^{\mathrm{b}}M\leq\beta_{n,t}^{\mathrm{b}}\leq\mu_{n,t}^{\mathrm{b}}M\\
&-\mu_{n,t}^{+}M\leq\beta_{n,t}^{+}\leq\mu_{n,t}^{+}M\\
&-\mu_{n,t}^{-}M\leq\beta_{n,t}^{-}\leq\mu_{n,t}^{-}M\\
&-\kappa_{n,t}^{\mathrm{b}}M\leq\gamma_{n,t}^{\mathrm{b}}\leq\kappa_{n,t}^{\mathrm{b}}M\\
&-\kappa_{n,t}^{+}M\leq\gamma_{n,t}^{+}\leq\kappa_{n,t}^{+}M\\
&-\kappa_{n,t}^{-}M\leq\gamma_{n,t}^{-}\leq\kappa_{n,t}^{-}M \qquad (40)
\end{aligned}
$$

The nonlinear term $\lambda_{n,t}^{rP}\left(U_{n,t}^{W}-U_{n,t}^{D}\right)$ in (37) is linearized as in (39) and (40) through the similar big-M based methods in [43] and [44]. For wind power uncertainty, $\beta_{n,t}^{\mathrm{base}}$, $\beta_{n,t}^{+}$ and $\beta_{n,t}^{-}$ are auxiliary continues variables corresponding to situations when $U_{n,t}^{W}$ takes the forecasted value, the upper bound and the lower bound. $\mu_{n,t}^{\mathrm{b}}$, $\mu_{n,t}^{+}$ and $\mu_{n,t}^{-}$are the auxiliary binary variables. M is a large enough positive number. The same method is used to deal with the power load uncertainty. The transformed sub-problem is a linear programming problem which can be solved by commercial solver.

To sum up, the algorithm for solving the model established in this paper is shown in Figure 4.

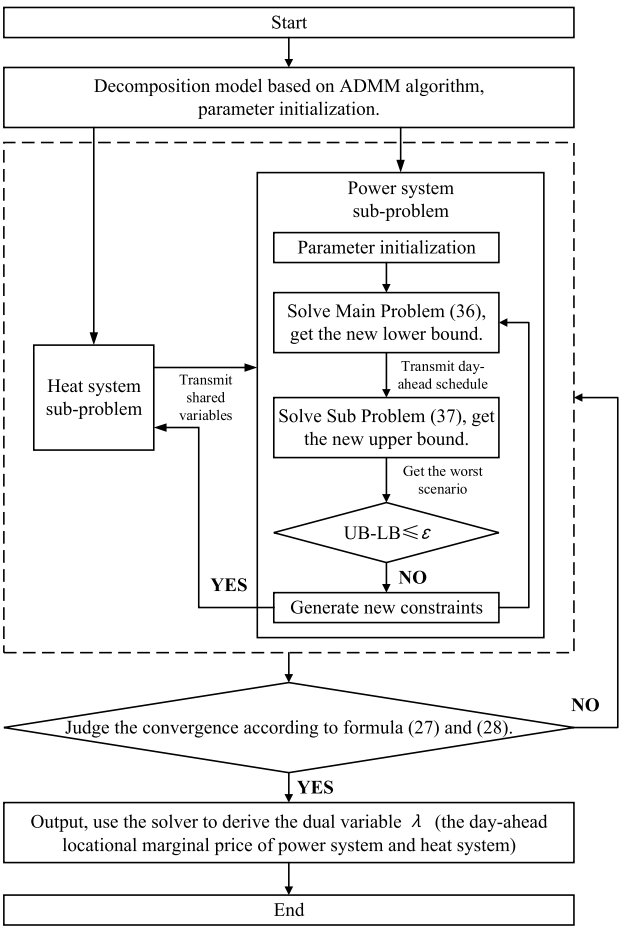

FIGURE 4. Flow chart of the algorithm.

IV. CASE STUDY

In this paper, based on the modified PJM-5 bus regional transmission network [45] and 32 node heating network [46], the simulation is carried out. The capacity and marginal cost of generator units including generator set, electric boiler and ground source heat pump, and system network structure of the regional integrated heat-power system are shown in Figure 5. The branch parameters are shown in Table 1. The total power load, heating load and wind power generation of the integrated system in each period are shown in Figure 6. Wind farms are set at power system bus 2 and bus 5. The power load is in the low valley at night, while the heating load and wind power generation are in the peak period. The cost of wind curtailment is assumed to be 25 $/MWh. The regulation cost of real-time stage is 1.5 times of the day-ahead generation cost. The linear programming problem is coded in MATLAB environment with YALMIP interface[47] and solved by CPLEX12.6 [48] in Windows 10 operating system under the hardware environment that Intel(R) Core(TM) i7-4710HQ CPU@2.50GHz, 8GB RAM.

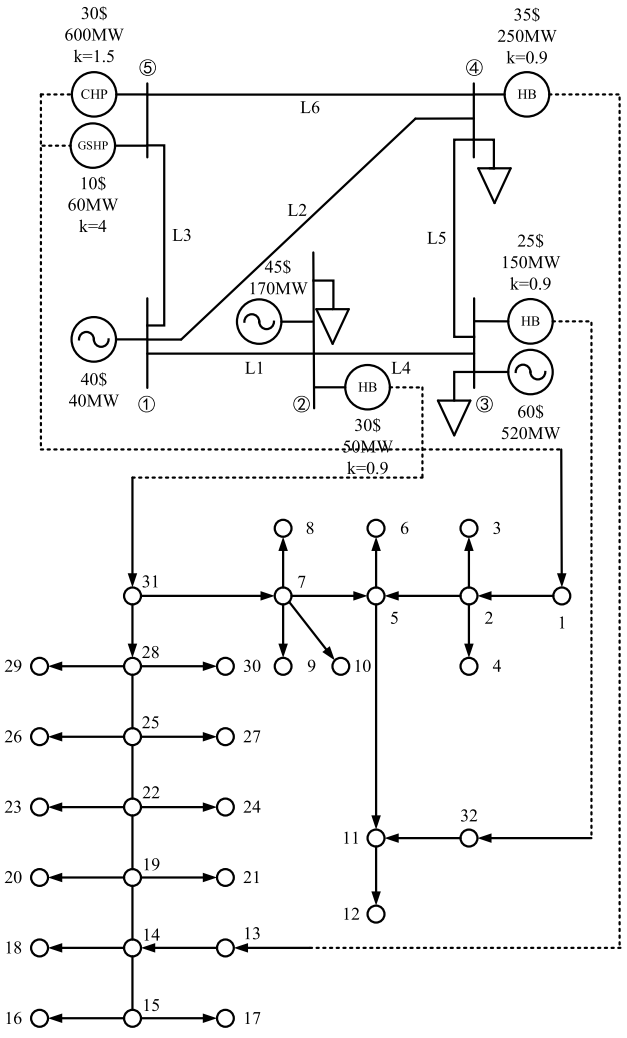

FIGURE 5. Structure diagram of 5 bus power system and 32 node heat system.

TABLE 1. Branch parameters.

Branch	L1	L2	L3	L4	L5	L6
R(%)	0.281	0.304	0.064	0.108	0.297	0.297
X(%)	2.81	3.04	0.64	1.08	2.97	2.97
$\overline{P_{ns}}$ (MW)	150	150	160	160	150	160

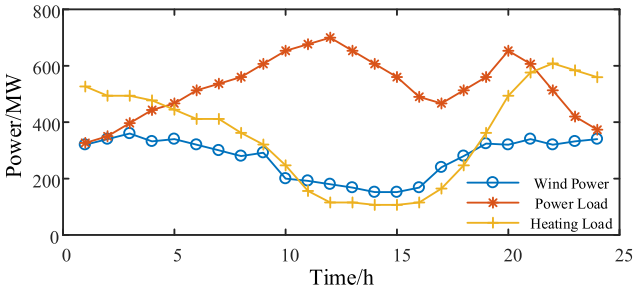

FIGURE 6. Curve of total power load, heating load and wind power generation of regional integrated heat-power system.

A. THE ROLE OF GSHP

In order to analyze the key role of the GSHP in the regional integrated heat-power system, the following two scenarios are set up in this paper:

(1) Scenario 1: There is no GSHP at bus 5 of power grid, and only EBs participate in wind power accommodation.

(2) Scenario 2: There is a GSHP at bus 5 of power grid, which participates in wind power accommodation together with EBs.

It can be seen from Figure 7 that when there is no GSHP at bus 5 of the power grid, a large amount of wind is abandoned during the period of high wind power generation at night, and the abandoned wind power even reaches 100%. This is due to the peak heating load at night, during which CHP units need to bear a lot of heating load. Accordingly, CHP units will produce a lot of electric energy. At the same time, due to the low power load at night, the accommodation space of wind power is greatly compressed. These reasons lead to a large number of abandoned wind power in the system. It can be seen from Table 2 that when there is no GSHP, CHP units are forced to generate a large amount of electric energy while generating heat to meet the demand of heating load. Wind power cannot be used, resulting in high system operation cost and wind curtailment cost. When the GSHP is installed at bus 5, the GSHP cannot only consume electric

TABLE 2. The impact of the GSHP on system.

Scenario number	System operation cost/$	Wind curtailment cost/$	Total power generation of CHP unit/MW
Scenario 1	6.77×10^5	4.06×10^4	3621.0
Scenario 2	5.05×10^5	0	719.3

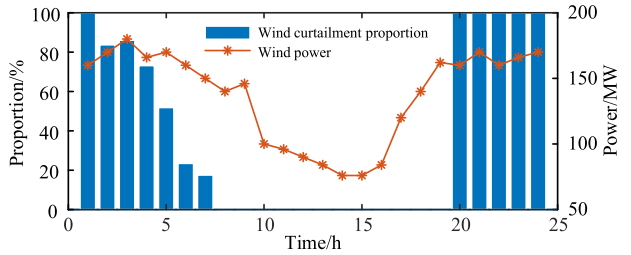

FIGURE 7. Wind power curtailment proportion of the system without the GSHP.

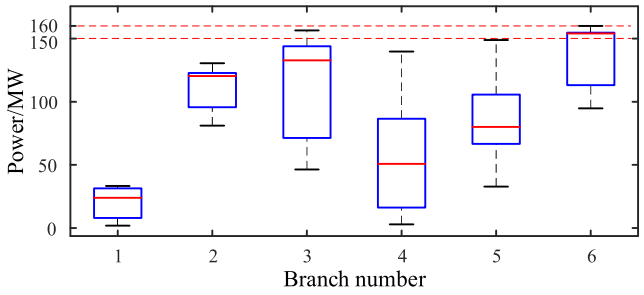

FIGURE 8. Branch power boxplot on power grid side in scenario 1 (the data for branches 3 and 6 are the inverse of their original data).

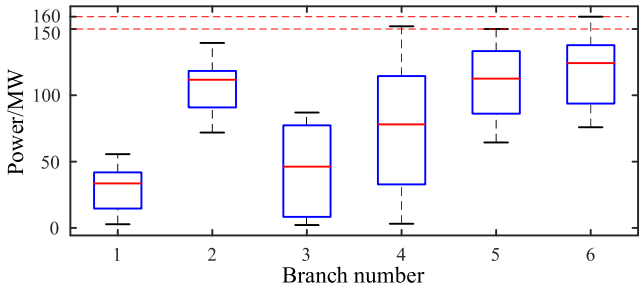

FIGURE 9. Branch power boxplot on power grid side in scenario 2 (the data for branches 3 and 6 are the inverse of their original data).

energy and provide accommodation space for the wind power on the power grid side, but also take the place of CHP units to bear a part of the heat load and reduce the power generation of CHP units. Based on this, the system can make full use of wind power to reduce operating costs, and the problem of wind power accommodation is also solved.

In addition, a large amount of wind power at bus 5 needs to be accommodated, but there is no power load that can participate in the wind power accommodation. Therefore, a large amount of power needs to be transmitted to the adjacent bus of bus 5 through branches L3 and L6. As can be seen in Figure 8, since there is no GSHPs to help CHP units share the heating load, the power generated by CHP units and wind power need to be transmitted from bus 5, resulting in that the transmission power of branch L3 and L6 in scenario 1 is very close to the maximum transmission power of branch in most periods. In scenario 2 with a GSHP installed, the transmission pressure of branch L3 and L6 is significantly reduced. It can be seen that the addition of GSHP can alleviate the branch transmission pressure caused by wind power accommodation.

B. PRICING STRATEGY FOR THE REGIONAL INTEGRATED HEAT-POWER SYSTEM

In order to analyze the impact of the uncertainty of wind power generation and power load on the locational marginal price of the regional integrated heat-power system, the following two scenarios are set up in this paper:

(1) Scenario 1: Wind power generation and power load are determined values, that is, system operators can accurately predict the power load and heating load demand in the next day.

(2) Scenario 2: Wind power generation and power load are uncertain, and the fluctuation range is $\pm 10\%$.

In order to avoid the occurrence of line congestion, the system operator should consider how to guide users to reduce the energy consumption during peak load period when setting the locational marginal price. The most ideal situation is to shift the power load as much as possible to the nighttime with high wind power generation, so as to improve the accommodation space of wind power. Taking bus 2 and bus 5 on the power grid side and node 3 on the heating network side as an example in Figure 10, under the deterministic condition, in order to achieve its purpose, the system operator will make the heat price higher in the nighttime period than in the daytime, and the electricity price lower in the nighttime period than in the daytime, so as to guide the heating load and power load to shift to the daytime and nighttime respectively through the price signal.

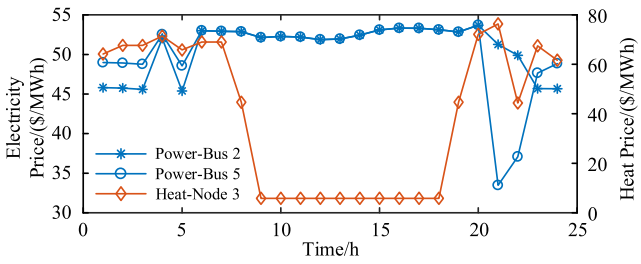

FIGURE 10. LMP of partial buses/nodes under the deterministic condition.

Under the condition of uncertainty, system operator need to consider the possible worst case. For the nighttime period, the worst-case scenario is obviously that the wind power generation is higher than the forecasted value and the power load is lower than the forecasted value as shown in the Figure 11 and 12. At this point, the accommodation space of wind power is compressed, resulting in an increased probability of wind power abandonment. Therefore, it can be seen from Figure 13 that the price gap between day and night is increasing. There are even peak price and negative price in the electricity price curve. The peak price is the upward and downward regulation cost caused by the uncertainty of the real-time stage. The emergence of negative price shows that

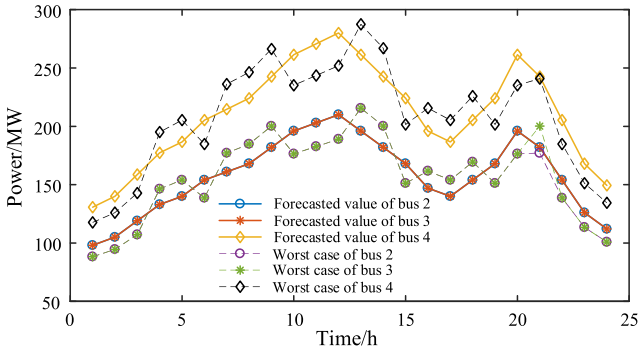

FIGURE 11. Load forecasted and worst value of bus 2-4.

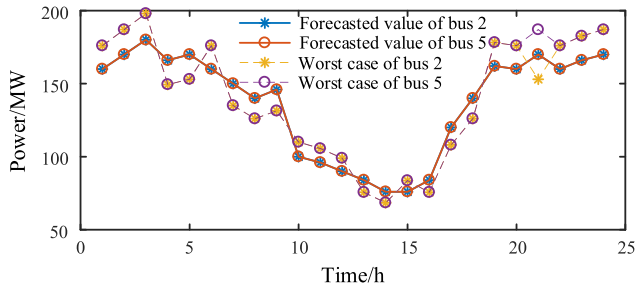

FIGURE 12. Wind power forecasted and worst value of bus 2 and 5.

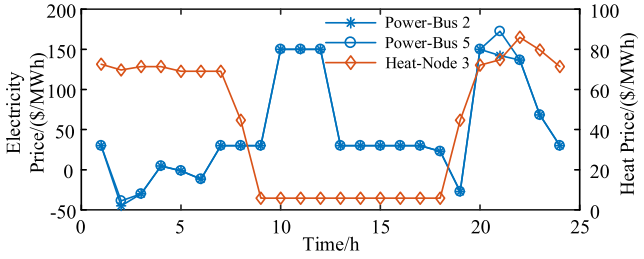

FIGURE 13. LMP of partial buses/nodes under uncertainty.

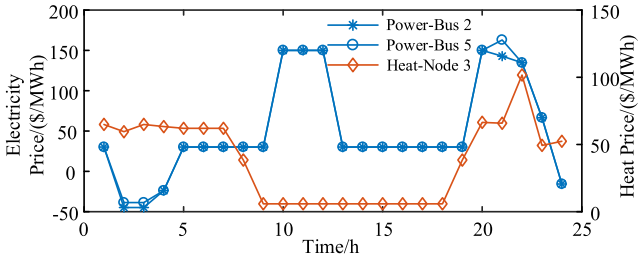

FIGURE 14. LMP of partial buses/nodes under uncertainty when k_{CHP} =1.2.

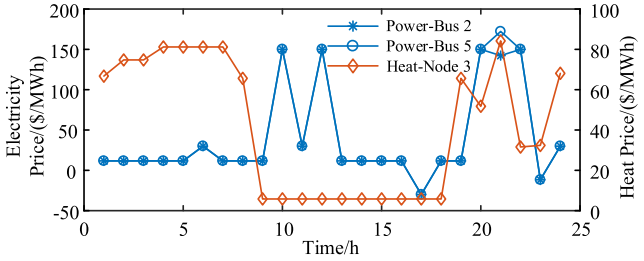

FIGURE 15. LMP of partial buses/nodes under uncertainty when k_{CHP} =2.0.

the system operator is eager to shift the daytime load to the nighttime as much as possible.

In addition to the uncertainty from wind power and power load will have an impact on the pricing strategy of the regional integrated heat-power system operator, the key coupling node of power grid and heating network, namely the cogeneration unit, its ratio of power generation and heat generation will also have an impact on the pricing strategy of the system operator. In this paper, the pricing strategies of the system operator are simulated under the conditions of k_{CHP} =1.2 and k_{CHP} =2.0. The numerical simulation results are shown in Figure 14 and 15. Comparing with Figure 13 to Figure 15, it can be concluded that with the increase of CHP unit coefficient k_{CHP}, the difference between peak and valley price will increase. This conclusion is more obvious in the heat price. The reason is that when the coefficient k_{CHP} of the CHP unit increases, it means that more electric power will be generated when the unit heat energy is produced, which will occupy the accommodation space of wind power. Therefore, the pricing strategy of the system operator is still to transfer the power load in the daytime to the nighttime as much as possible, and the heat load in the nighttime to the daytime as much as possible. The larger the k_{CHP} value is, the more urgent the demand of the system operator will be.

C. IMPACT AND SOLUTIONS OF BRANCH CONGESTION

The strong heat demand in the heat system at night will make the CHP units in the power system generate a large amount of electricity correspondingly. The transmission of these electricity is likely to lead to the line congestion. In order to analyze the impact on the locational marginal price of the regional integrated heat-power system when the branch transmission power is insufficient, and the effect of some solutions to congestion, the following four scenarios are set up in this paper:

(1) Scenario 1: The transmission capacity of branch L6 is reduced to 150MW, and other conditions remain unchanged.

(2) Scenario 2: The transmission capacity of branch L6 is reduced to 150MW and the capacity of GSHP is increased to 80MW.

(3) Scenario 3: The transmission capacity of branch L6 is reduced to 150MW and set the CHP unit coefficient k_{CHP} =1.2.

(4) Scenario 4: The transmission capacity of branch L6 is reduced to 150MW, and set the GSHP coefficient η^{GSHP} =5.

From the calculation results of Scenario 1 in Table 3, it can be seen that when the transmission capacity of branch L6 is reduced, the wind curtailment proportion in the system and the system operation cost are increased. At the same time, in Figure 16 to 20, the more serious line congestion makes the

TABLE 3. Calculation results under different scenarios.

Scenario number	System operation cost/$	Wind curtailment cost/$
Scenario 1	5.22×10^5	1.29×10^3
Scenario 2	4.97×10^5	0
Scenario 3	5.09×10^5	9.2×10^2
Scenario 4	5.04×10^5	0

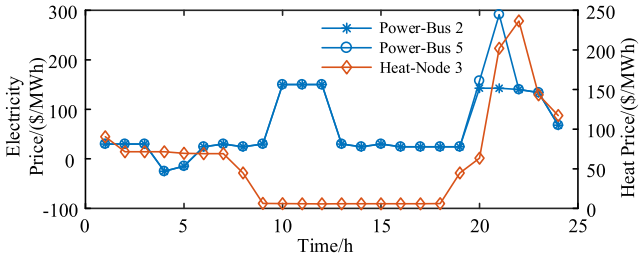

FIGURE 16. LMP of partial buses/nodes in scenario 1.

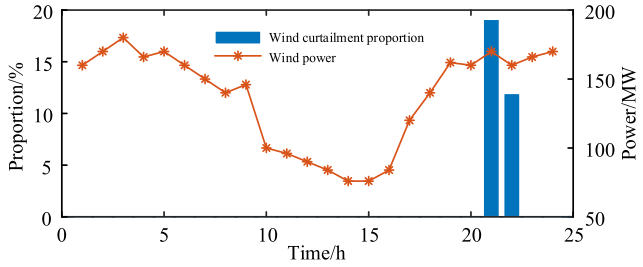

FIGURE 17. Wind power curtailment proportion of the system in scenario 1.

congestion price part of LMP at bus 4 increase significantly at 20:00 and 21:00.

In scenario 2 to 4, increasing the capacity of GSHPs, reducing the proportional coefficient of CHPs and increasing the energy conversion coefficient of GSHPs are used to solve the problems caused by the decrease of branch transmission capacity respectively. These three methods are marked as M1, M2 and M3 sequentially. The function of M1 and M3 is to increase the power consumption in the power system, while M2 is to reduce the output of the generation units. In essence, they all increase the space for wind power accommodation. From the final effect of all improvement methods:

1) All these methods enable the system to absorb more wind power to reduce the system operation cost;

2) M1 and M3 can reduce the wind curtailment proportion to zero, but M2 cannot. The reason is that the proportional coefficient of CHPs can be reduced in a limited range;

3) Since only GSHP acts as the power load at bus 5, a large amount of power generated by the CHP needs to be transmitted to bus 1 and 4 through branches L3 and L6 respectively. However, there is no load at bus 1. Only a small amount of power is transmitted on L3, and a large amount of power is transmitted on L6. This results in the branch L6 operating at maximum transmission power in all scenarios during the peak heat demand period at night. Therefore, the congestion problem in all scenarios cannot be solved under the set conditions, and the electricity price at 20:00 and 21:00 increased significantly due to congestion. Continuing to increase the capacity of the GSHPs may solve the congestion. However, investing too much GSHPs in the actual system requires further study.

4) All methods reduce the pressure of guiding users to use more heat at night on the heat system side by reducing the amount of electricity generated when generating the same amount of heat and consuming more electricity to generate the same amount of heat. Therefore, the differences between peak and valley price of heat price in Figures 18 to 20 are less than that in Figure 16.

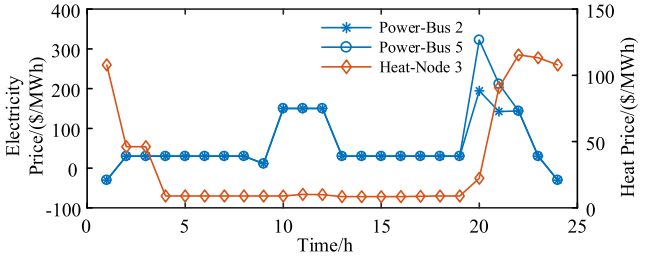

FIGURE 18. LMP of partial buses/nodes in scenario 2.

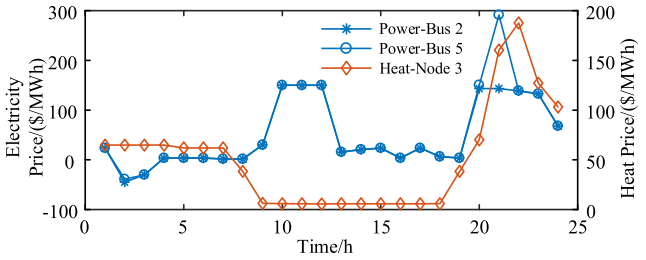

FIGURE 19. LMP of partial buses/nodes in scenario 3.

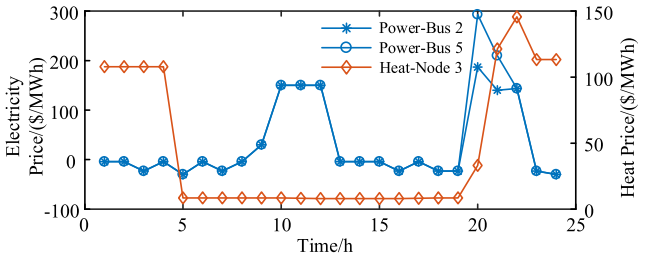

FIGURE 20. LMP of partial buses/nodes in scenario 4.

D. CONVERGENCE ANALYSIS OF ALGORITHM

The convergence of C&CG algorithm and ADMM algorithm is shown in Figure 16. It can be seen that every time C&CG algorithm is called to solve the two-stage robust optimization problem, the curve tends to be stable after the fourth iteration. ADMM algorithm also converges after the fourth iteration. During the simulation process, the consuming time of heat system problem (HSP), power system main problem (PSMP) and sub-problem (PSSP) and the whole problem are shown in Table 4.

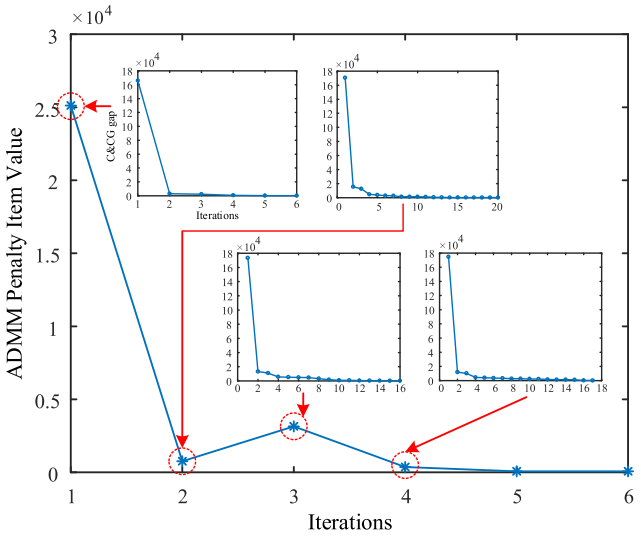

FIGURE 21. Convergence of the algorithm.

TABLE 4. Consuming time of each step when the transmission capacity of branch L6 is 160MW.

Iteration Number	HSP(s)	PSMP(s)	PSSP(s)	Whole Problem(s)*
1	2.221	4.674	9.738	17.414
2	1.946	18.072	73.294	93.993
3	1.465	14.954	28.121	45.764
4	1.535	15.181	29.164	47.109
5	1.986	21.992	37.825	63.626
6	1.217	19.486	26.606	49.222
Total	10.369	94.359	204.748	317.128

* Consuming time of data initialization/output is included.

TABLE 5. Consuming time of each step when the transmission capacity of branch L6 are 150MW and 180MW.

Transmission capacity	Total iterations	HSP(s)	PSMP(s)	PSSP(s)	Whole Problem(s)
150	12	14.910	693.149	747.347	1463.224
180	6	8.056	25.258	46.049	86.153

More importantly, by comparing Table 4 and V, it can be seen that the solution can be quickly completed when the branch transmission capacity in the power system is sufficient. However, when there is insufficient transmission capacity, the total iteration number and consuming time increase. Therefore, whether the transmission capacity of the branches in the power system is sufficient or not has a great impact on the algorithm convergence speed. But in general, the distributed algorithm for solving the two-stage robust optimization model of the regional integrated heat-power system is feasible and has good convergence.

V. CONCLUSION

In order to solve the wind abandonment problem during the high wind power generation period at night, methods including installing GSHPs at CHP units and guidance based on price signal is proposed. Based on the two-stage robust optimization model of the regional integrated heat-power system established, the impact of uncertainties on the pricing strategy is analyzed. The conclusions are as follows:

(1) Reducing the power generation of CHP units can improve the accommodation space of wind power. The GSHPs can share a part of the heating load for CHP units to reduce the power generation of CHP units under the operation mode of "power determined by heat".

(2) Increasing the daytime heating load and reducing the nighttime power load are beneficial to the accommodation of nighttime wind power, which can be achieved by system operators using price signals. The greater the uncertainty of power load and the proportional coefficient of CHP units, the greater the gap between daytime and nighttime LMP.

(3) Methods including increasing the capacity of GSHPs, reducing the proportional coefficient of CHPs and increasing the energy conversion coefficient of GSHPs can be used to solve the wind power abandonment problem caused by the insufficient transmission capacity.

(4) The distributed algorithm proposed is feasible and has good convergence. It can solve the model quickly when the branch transmission capacity is sufficient. When the branch transmission power in the power system is insufficient, the iteration number and the consuming time increase.

In this paper, the heating load at each node is only calculated in terms of the total amount, not a refined model. However, similar to the GSHPs, the thermal inertia of the distributed heating networks and buildings can bring a lot of flexible resources to the heat system [49], [50]. Through using these flexible resources, the heating load curve can be improved, and then the output of CHP units can be optimized to improve the accommodation space of wind power. In addition, the energy preferences of users will bring uncertainty to the heating load [32]. These are promising research directions. Further research will be carried out in this direction in future work. Based the study results in this paper, the following assumptions can be made: 1) The thermal inertia can improve the wind power accommodation capacity of the system, which may be more flexible than the GSHPs; 2) When heating load is uncertain, the operator will increase and decrease the heat price during the nighttime and daytime respectively to shift the heating load to the daytime. The increase of uncertainty range will increase the gap between the peak and valley prices.

REFERENCES

[1] (2019). *Emissions Gap Report 2019*. [Online]. Available: https://www.unep.org/resources/emissions-gap-report-2019
[2] (2020). *Emissions Gap Report 2020*. [Online]. Available: https://www.unep.org/emissions-gap-report-2020
[3] (2021). *Wind Power in Denmark*. [Online]. Available: https://en.wikipedia.org/wiki/Wind power in Denmark
[4] (2016). *Energy Department Reports*. [Online]. Available: https://www.energy.gov/articles/energy-department-reportswind-energy-continues-rapid-growth-2016
[5] (2017). *ERCOT Reaches 50% Wind Penetration Mark*. [Online]. Available: https://www.rtoinsider.com/ercot-wind-penetration-40749

[6] L. Che, X. Liu, X. Zhu, M. Cui, and Z. Li, "Intra-interval security assessment in power systems with high wind penetration," *IEEE Trans. Sustain. Energy*, vol. 10, no. 4, pp. 1890–1903, Oct. 2019, doi: 10.1109/TSTE.2018.2875148.

[7] X. Wu and Y. Jiang, "Source-network-storage joint planning considering energy storage systems and wind power integration," *IEEE Access*, vol. 7, pp. 137330–137343, Sep. 2019, doi: 10.1109/ACCESS.2019.2942134.

[8] Y. Zhang, X. Han, B. Xu, M. Wang, P. Ye, and Y. Pei, "Risk-based admissibility analysis of wind power integration into power system with energy storage system," *IEEE Access*, vol. 6, pp. 57400–57413, 2018, doi: 10.1109/ACCESS.2018.2870736.

[9] M. Zhou, M. Wang, J. F. Li, and G. Y. Li, "Multi-area generation-reserve joint dispatch approach considering wind power cross-regional accommodation," *CSEE J. Power Energy Syst.*, vol. 3, no. 1, pp. 74–83, Mar. 2017, doi: 10.17775/CSEEJPES.2017.0010.

[10] Q. Xu, N. Zhang, C. Kang, Q. Xia, D. He, C. Liu, Y. Huang, L. Cheng, and J. Bai, "A game theoretical pricing mechanism for multi-area spinning reserve trading considering wind power uncertainty," *IEEE Trans. Power Syst.*, vol. 31, no. 2, pp. 1084–1095, Mar. 2016, doi: 10.1109/TPWRS.2015.2422826.

[11] W. Linjun, L. Yan, C. Yongning, W. Zhen, and B. Hong, "Research on market mechanism of wind power accommodation based on power bidding," in *Proc. Int. Conf. Power Syst. Technol.*, Oct. 2014, pp. 2623–2628. [Online]. Available: https://ieeexplore.ieee.org/document/6993590

[12] H. M. Hussain, A. Narayanan, P. H. J. Nardelli, and Y. Yang, "What is energy internet? Concepts, technologies, and future directions," *IEEE Access*, vol. 8, pp. 183127–183145, Oct. 2020, doi: 10.1109/ACCESS.2020.3029251.

[13] B. Fang, B. Wang, and D. W. Gao, "Optimal operation strategy considering wind power accommodation in heating district," in *Proc. North Amer. Power Symp. (NAPS)*, Sep. 2016, pp. 1–5. [Online]. Available: https://ieeexplore.ieee.org/document/7747891

[14] L. Jian, C. Shanshan, B. Cunxi, L. Hairong, L. Feng, and Z. Xiaodong, "Research on effect of wind curtailment accommodation for combined heat and power units with heat storage," in *Proc. Int. Conf. Eng. Simul. Intell. Control (ESAIC)*, Aug. 2018, pp. 68–72. [Online]. Available: https://ieeexplore.ieee.org/document/8530366

[15] B. Liu, J. Li, S. Zhang, M. Gao, H. Ma, G. Li, and C. Gu, "Economic dispatch of combined heat and power energy systems using electric boiler to accommodate wind power," *IEEE Access*, vol. 8, pp. 41288–41297, Jan. 2020, doi: 10.1109/ACCESS.2020.2968583.

[16] T. Jiang, Y. Min, W. C. Ge, L. Chen, Q. Chen, F. Xu, H. H. Luo, and G. P. Zhou, "Hierarchical dispatch method for integrated heat and power systems based on a feasible region of boundary variables," *CSEE J. Power Energy Syst.*, vol. 6, no. 3, pp. 543–553, Sep. 2020, doi: 10.17775/CSEEJPES.2019.02930.

[17] Z. Chen, G. Zhu, Y. Zhang, T. Ji, Z. Liu, X. Lin, and Z. Cai, "Stochastic dynamic economic dispatch of wind-integrated electricity and natural gas systems considering security risk constraints," *CSEE J. Power Energy Syst.*, vol. 5, no. 3, pp. 324–334, Sep. 2019, doi: 10.17775/CSEEJPES.2019.00150.

[18] D. D'Agostino, L. Mele, F. Minichiello, and C. Renno, "The use of ground source heat pump to achieve a net zero energy building," *Energies*, vol. 13, no. 13, p. 3450, Jul. 2020, doi: 10.3390/en13133450.

[19] B. Emanuele and A. Andrea, "Life-cycle assessment of an innovative ground-source heat pump system with upstream thermal storage," *Energies*, vol. 10, no. 11, p. 1854, Nov. 2017, doi: 10.3390/en10111854.

[20] H. Huan, L. Kai, J. Shaoyu, L. Xiaoyang, L. Bo, L. Yang, J. Yilin, and G. Dandan, "Research on optimized operation of electrothermal combined system for enhancing wind power consumption," in *Proc. 3rd Int. Conf. Smart City Syst. Eng. (ICSCSE)*, Dec. 2018, pp. 631–635. [Online]. Available: https://ieeexplore.ieee.org/document/8705540

[21] G. M. Tseyzer, O. S. Ptashkina-Girina, and G. N. Ryavkin, "Development of mathematical model of joint work of heat pump and cogeneration power plant," in *Proc. Int. Ural Conf. Electr. Power Eng. (UralCon)*, Sep. 2020, pp. 82–86. [Online]. Available: https://ieeexplore.ieee.org/document/8705540

[22] K. Gao, L. Zhao, C. Wang, P. Qiu, and N. Meng, "Economic analysis of combined cooling, heating and power system coupled with heat pump based on EnergyPLAN," in *Proc. Chin. Autom. Congr. (CAC)*, Nov. 2020, pp. 7268–7272. [Online]. Available: https://ieeexplore.ieee.org/document/8705540

[23] Y. Cao, W. Wei, L. Wu, S. Mei, M. Shahidehpour, and Z. Li, "Decentralized operation of interdependent power distribution network and district heating network: A market-driven approach," *IEEE Trans. Smart Grid*, vol. 10, no. 5, pp. 5374–5385, Sep. 2019, doi: 10.1109/TSG.2018.2880909.

[24] N. Arcuri, R. Bruno, and C. Carpino, "PV driven heat pumps for the electric demand-side management: Experimental results of a demonstrative plant," in *Proc. IEEE Int. Conf. Environ. Electr. Eng. IEEE Ind. Commercial Power Syst. Eur. (EEEIC/I&CPS Europe)*, Jun. 2018, pp. 1–8. [Online]. Available: https://ieeexplore.ieee.org/document/8705540

[25] (2021). *PJM-Home*. [Online]. Available: https://www.pjm.com/

[26] P. M. Sotkiewicz and J. M. Vignolo, "Nodal pricing for distribution networks: Efficient pricing for efficiency enhancing DG," *IEEE Trans. Power Syst.*, vol. 21, no. 2, pp. 1013–1014, May 2006, doi: 10.1109/TPWRS.2006.873006.

[27] R. K. Singh and S. K. Goswami, "Optimum allocation of distributed generations based on nodal pricing for profit, loss reduction, and voltage improvement including voltage rise issue," *Int. J. Electr. Power Energy Syst.*, vol. 32, no. 6, pp. 637–644, Jul. 2010, doi: 10.1016/j.ijepes.2009.11.021.

[28] F. Meng and B. H. Chowdhury, "Distribution LMP-based economic operation for future smart grid," in *Proc. IEEE Power Energy Conf. at Illinois*, Feb. 2011, pp. 1–5. [Online]. Available: https://ieeexplore.ieee.org/document/5740485

[29] Y. Chen, W. Wei, F. Liu, E. E. Sauma, and S. Mei, "Energy trading and market equilibrium in integrated heat-power distribution systems," *IEEE Trans. Smart Grid*, vol. 10, no. 4, pp. 4080–4094, Jul. 2019, doi: 10.1109/TSG.2018.2849227.

[30] X. Fang, B.-M. Hodge, E. Du, C. Kang, and F. Li, "Introducing uncertainty components in locational marginal prices for pricing wind power and load uncertainties," *IEEE Trans. Power Syst.*, vol. 34, no. 3, pp. 2013–2024, May 2019, doi: 10.1109/TPWRS.2018.2881131.

[31] S. Lu, W. Gu, S. Zhou, S. Yao, and G. Pan, "Adaptive robust dispatch of integrated energy system considering uncertainties of electricity and outdoor temperature," *IEEE Trans. Ind. Informat.*, vol. 16, no. 7, pp. 4691–4702, Jul. 2020, doi: 10.1109/TII.2019.2957026.

[32] S. Lu, W. Gu, K. Meng, and Z. Dong, "Economic dispatch of integrated energy systems with robust thermal comfort management," *IEEE Trans. Sustain. Energy*, vol. 12, no. 1, pp. 222–233, Jan. 2021, doi: 10.1109/TSTE.2020.2989793.

[33] S. Surender Reddy, P. R. Bijwe, and A. R. Abhyankar, "Real-time economic dispatch considering renewable power generation variability and uncertainty over scheduling period," *IEEE Syst. J.*, vol. 9, no. 4, pp. 1440–1451, Dec. 2015, doi: 10.1109/JSYST.2014.2325967.

[34] S. S. Reddy, "Optimal scheduling of thermal-wind-solar power system with storage," *Renew. Energy*, vol. 101, pp. 1357–1368, Feb. 2017, doi: 10.1016/j.renene.2016.10.022.

[35] S. S. Reddy and J. A. Momoh, "Realistic and transparent optimum scheduling strategy for hybrid power system," *IEEE Trans. Smart Grid*, vol. 6, no. 6, pp. 3114–3125, Nov. 2015, doi: 10.1109/TSG.2015.2406879.

[36] D. Maity, A. Chowdhury, S. S. Reddy, B. K. Panigrahi, A. R. Abhyankar, and M. K. Mallick, "Joint energy and spinning reserve dispatch in wind-thermal power system using IDE-SAR technique," in *Proc. IEEE Symp. Swarm Intell. (SIS)*, Apr. 2013, pp. 284–290. [Online]. Available: https://ieeexplore.ieee.org/document/6615191

[37] S. S. Reddy and J. A. Momoh, "Minimum emissions optimal power flow in wind-thermal power system using opposition based bacterial dynamics algorithm," in *Proc. IEEE Power Energy Soc. Gen. Meeting (PESGM)*, Jul. 2016, pp. 1–5. [Online]. Available: https://ieeexplore.ieee.org/document/7741635/citations#citations

[38] S. M. Nosratabadi, M. Jahandide, and J. M. Guerrero, "Robust scenario-based concept for stochastic energy management of an energy hub contains intelligent parking lot considering convexity principle of CHP nonlinear model with triple operational zones," *Sustain. Cities Soc.*, vol. 68, May 2021, Art. no. 102795, doi: 10.1016/j.scs.2021.102795.

[39] H. Zafarani, S. A. Taher, and M. Shahidehpour, "Robust operation of a multicarrier energy system considering EVs and CHP units," *Energy*, vol. 192, Feb. 2020, Art. no. 116703, doi: 10.1016/j.energy.2019.116703.

[40] S. Nojavan, A. Akbari-Dibavar, A. Farahmand-Zahed, and K. Zare, "Risk-constrained scheduling of a CHP-based microgrid including hydrogen energy storage using robust optimization approach," *Int. J. Hydrogen Energy*, vol. 45, no. 56, pp. 32269–32284, Nov. 2020, doi: 10.1016/j.ijhydene.2020.08.227.

[41] S. Boyd, N. Parikh, E. Chu, B. Peleato, and J. Eckstein, "Distributed optimization and statistical learning via the alternating direction method of multipliers," *Found. Trends Mach. Learn.*, vol. 3, no. 1, pp. 1–122, Jan. 2011, doi: 10.1561/2200000016.
[42] C. Shao, X. Wang, X. Wang, C. Du, and B. Wang, "Hierarchical charge control of large populations of EVs," *IEEE Trans. Smart Grid*, vol. 7, no. 2, pp. 1147–1155, Mar. 2016, doi: 10.1109/TSG.2015.2396952.
[43] T. Ding, S. Liu, W. Yuan, Z. Bie, and B. Zeng, "A two-stage robust reactive power optimization considering uncertain wind power integration in active distribution networks," *IEEE Trans. Sustain. Energy*, vol. 7, no. 1, pp. 301–311, Jan. 2016, doi: 10.1109/TSTE.2015.2494587.
[44] H. Ji, C. Wang, P. Li, F. Ding, and J. Wu, "Robust operation of soft open points in active distribution networks with high penetration of photovoltaic integration," *IEEE Trans. Sustain. Energy*, vol. 10, no. 1, pp. 280–289, Jan. 2019, doi: 10.1109/TSTE.2018.2833545.
[45] F. Li and R. Bo, "DCOPF-based LMP simulation: Algorithm, comparison with ACOPF, and Sensitivity," *IEEE Trans. Power Syst.*, vol. 22, no. 4, pp. 1475–1485, Nov. 2007, doi: 10.1109/TPWRS.2007.907924.
[46] X. Liu, J. Wu, N. Jenkins, and A. Bagdanavicius, "Combined analysis of electricity and heat networks," *Appl. Energy*, vol. 162, pp. 1238–1250, Jan. 2016, doi: 10.1016/j.apenergy.2015.01.102.
[47] (2021). *YALMIP*. [Online]. Available: https://yalmip.github.io/
[48] (2021). *CPLEX Optimizer*. [Online]. Available: https://www.ibm.com/analytics/cplex-optimizer
[49] S. Lu, W. Gu, K. Meng, S. Yao, B. Liu, and Z. Y. Dong, "Thermal inertial aggregation model for integrated energy systems," *IEEE Trans. Power Syst.*, vol. 35, no. 3, pp. 2374–2387, May 2020, doi: 10.1109/TPWRS.2019.2951719.
[50] S. Lu, W. Gu, S. Zhou, W. Yu, and G. Pan, "High-resolution modeling and decentralized dispatch of heat and electricity integrated energy system," *IEEE Trans. Sustain. Energy*, vol. 11, no. 3, pp. 1451–1463, Jul. 2020, doi: 10.1109/TSTE.2019.2927637.

DONGMEI YANG received the bachelor's degree in engineering from the School of Electrical Engineering, Sichuan University, in 2004, and the master's degree in engineering from the Nanjing Automation Research Institute of State Grid, in 2007. She is currently the Director of Technical Research Center of NARI Research Institute, NARI Group (State Grid Electric Power Research Institute). Her main research interests include integrated energy system modeling and simulation, energy storage system integration and energy management, and cold and heat storage technology.

ZHIHONG YANG received the bachelor's degree from Computer Department, Nanjing University, in 1990, and the master's degree in computer science and technology from the School of Computer Science, Southeast University, in 1998. He is currently the Vice President of NARI Research Institute, NARI Group (State Grid Electric Power Research Institute). His main research interests include operation optimization of integrated energy systems, power system automation, new energy power generation, and computer application technology.

GUOXIN HE received the bachelor's degree in engineering from the School of Electrical Engineering, Sichuan University, in 2015. He is currently pursuing the master's degree with the NARI College of Electrical and Automation Engineering. He is also a Research Engineer with Technology Research Center of NARI Research Institute, NARI Group (State Grid Electric Power Research Institute). His main research interests include battery energy storage system integration and control, integrated energy system modeling and simulation, planning and operation, and information physical systems.

JIAN GENG received the bachelor's degree in engineering from the School of Chemical Engineering, China University of Mining and Technology, in 2015, and the master's degree in engineering from the School of Energy and Environment, Southeast University, in 2018. He is currently a Research and Development Engineer of Technology Research Center of NARI Research Institute, NARI Group (State Grid Electric Power Research Institute). His main research interests include integrated energy system daily scheduling, micro gas turbine control, cooling heating, and power triple generation system modeling and control.

JUNJIE LIGAO (Member, IEEE) was born in Guangxi, China, in 1996. He received the B.S. degree in electrical engineering from Chongqing University, Chongqing, China, in 2018. He is currently pursuing the Ph.D. degree in electrical engineering with the School of Electrical Engineering and Automation, Wuhan University, China. His research interests include energy integrated power system operation and power grid planning.